V International Conference on Computational Methods for Coupled Problems in Science and Engineering
COUPLED PROBLEMS 2013
S. Idelsohn, M. Papadrakakis and B. Schrefler (Eds)

NUMERICAL SIMULATION OF EXPLOSIVE FRACTURING WITH SMOOTHED PARTICLE HYDRODYNAMICS

ZHIMING GUO[*,†], YONGXING SHEN[*] AND MOUBIN LIU[‡]

[*]Laboratori de Càlcul Numèric (LaCàN)
Universitat Politècnica de Catalunya (UPC BarcelonaTech)
C/ Jordi Girona 1-3, Campus Nord, 08034 Barcelona, Spain
Email: guozhiming@live.cn (Guo), yongxing.shen@upc.edu (Shen)
Web page: http://www.lacan.upc.edu/

[†]School of Mechatronic Engineering
North University of China
Xueyuan Road 3, 030051 Taiyuan, Shanxi, China
E-mail: guozhiming@live.cn - Web page: http://www.nuc.edu.cn/

[‡]Key Laboratory for Mechanics in Fluid Solid Coupling Systems
Institute of Mechanics, Chinese Academy of Sciences
#15, Bei Si Huan Xi Lu, Haidian District, Beijing, China 100190
Email: liumoubin@imech.ac.cn - Web page: http://lmfs.imech.cas.cn//

Key words: Explosive Fracture, Smoothed Particle Hydrodynamics, Elasto-damage Model, Rock Fracture, Meshfree Method

Abstract. In this paper we study explosive fracturing with smoothed particle hydrodynamics (SPH). As a particle based Lagrangian method, SPH is particularly suited to the analysis of fracture due to its full Lagrangian frame and capacity to model large deformation. We adopt the Jones-Wilkins-Lee equation as equation of state of the trinitrotoluene (TNT) explosive and a continuum elasto-damage model to predict the fracture of the rock. We predict the evolution of damage using the strain history of each particle. To strengthen the interaction of coupling interfaces we use a penalty function to avoid penetration between different material particles.

1 INTRODUCTION

Explosive fracturing is an important approach in industries such as shale gas exploration, shale oil exploration, rock excavation, and mineral and ore processing. This technique has been effectively used by a few countries. Since the earliest days of blasting with black powder there have been steady developments in explosives, detonation and the

understanding of the mechanics of rock fracture by explosives, but the fundamental mechanisms of rock damage are not yet fully understood in many aspects. Hence, approaches for studying fracture have been heavily dependent on empirical relations based on experimental data of the laboratory scale. Duvall and Fogelson [1], Langefors and Khilstrom [2], and others have published blast damage criteria for buildings and other surface structures. All of these criteria relate blast damage to peak particle velocity resulting from the dynamic stresses induced by the explosion. Both the dynamic stresses induced by the detonation and the expanding gases produced by the explosion play important roles in the fragmentation process, but it is difficult to study the details about this mechanism.

On the other hand, numerical simulations, as an effective mean, can help understand and predict complex exploding and fracture processes. Of the many available methods, mesh-based methods seem inadequate in tracking the motions of the fragments. Instead, most existing methods for this problem fall in one of two categories of methods.

One category of methods, such as the discrete element method [3, 4], explicitly tracks the motion of fragments. Another category of methods models the solid as a damaging body, such as [5, 6, 7, 8, 9]. Damage inhibits the transmission of tensile stress between particles, and once it reaches unity, the particle is unable to transmit tensile stress, resulting in a macro-crack. Connected macro-cracks lead to complete fragmentation. We also mention here damage models for various kinds of solids [10, 11, 12, 13].

One possibility of discretizing the continuous equations of a damage model is to use the smoothed particle hydrodynamics (SPH). SPH was initially developed to solve astrophysical problems[14] Due to its special features and advantages, it has been applied to various areas in engineering and sciences [15].

In this paper, we study the explosive fracturing of rock mass with the SPH method. This process involves the explosion of TNT, the interaction of exploding gas and rock, and the fracture of rock. To model the rock, we employ a modified version of the Grady-Kipp model [16]. The SPH is suited for modeling explosive fracture because it is insensitive to disordered particle distribution, a consequence of the fast expansion of explosive gas and rapid deformation and fast damage on materials.

The rest of this work is organized as follows. In Section 2 we state the problem we want to solve and give the governing equations. In Section 3 we discretize these governing equations with the SPH method. Finally in Section 4 we verify our results by numerical examples.

2 PROBLEM STATEMENT

We study the damage of a piece of rock mass during the detonation and explosion of trinitrotoluene (TNT) explosive in a preexisting crack. For simplicity we will confine ourselves to two-dimensions (2D) within this work. In this section we will introduce the governing equations that model the coupled problem of explosive fracturing. In particular, Section 2.1 states the conservation laws and Section 2.2 gives the constitutive equations and equations of state for both phases: the damaging rock and the exploding gas.

2.1 Conservation laws

In the Langrangian frame, the motion of both the rock mass and the explosive is governed by the following conservation equations:

$$\begin{cases} \dfrac{Dx^\alpha}{Dt} = v^\alpha, \\ \dfrac{Dv^\alpha}{Dt} = \dfrac{1}{\rho}\dfrac{\partial \sigma_d^{\alpha\beta}}{\partial x^\beta}, \\ \dfrac{D\rho}{Dt} = -\rho\dfrac{\partial v^\beta}{\partial x^\beta}, \\ \dfrac{De}{Dt} = \dfrac{\sigma_d^{\alpha\beta}}{\rho}\dfrac{\partial v^\alpha}{\partial x^\beta}, \end{cases} \tag{1}$$

of which the first equation is the definition of the velocity, and the second, third, and fourth equations represent the conservation of momentum, mass and energy, respectively. Here superscripts $\alpha, \beta = 1, 2$ denote the component index in the Cartesian coordinates, for which repeated indices imply summation from 1 to 2. Quantities $\mathbf{x}$, $\mathbf{v}$, ρ, e, and $\boldsymbol{\sigma}_d$ are the position vector, velocity vector, density, energy, and the damaged (Cauchy) stress tensor, respectively. Among these, the damaged stress tensor describes the effect of the material damage in terms of a modification of the undamaged stress tensor $\boldsymbol{\sigma}$. Derivative D/Dt denotes the total derivative, or termed material derivative.

2.2 Constitutive equations and equations of state

Below we specify the constitutive equations and equations of state for the rock mass (Section 2.2.1) and the explosive gas (Section 2.2.2). In this part we closely follow [16].

2.2.1 The rock mass

In the sequel we first describe how we model the undamaged stress tensor $\boldsymbol{\sigma}$, and then detail how we take into account the damage effect.

The undamaged stress tensor. For the rock, the undamaged stress tensor consists of two parts:

$$\sigma^{\alpha\beta} = -P\delta^{\alpha\beta} + S^{\alpha\beta}, \tag{2}$$

where $\delta^{\alpha\beta}$ is the Kronecker delta, P is the elastic pressure, and $\boldsymbol{S}$ is the deviatoric stress tensor. We assume the elastic pressure is proportional to the change in density:

$$P = c^2(\rho - \rho_0), \tag{3}$$

where ρ_0 is the reference density, ρ is the current density and c is the longitudinal wave speed of the solid material.

On the other hand, we can express the deviatoric stress $\boldsymbol{S}$ with Hooke's law using the Jaumann rate equation [17]:

$$\frac{DS^{\alpha\beta}}{Dt} = 2G\left(\ell^{\alpha\beta} - \frac{1}{3}\ell^{\gamma\gamma}\delta^{\alpha\beta}\right) + S^{\alpha\gamma}\Omega^{\gamma\beta} - \Omega^{\alpha\gamma}S^{\gamma\beta}, \tag{4}$$

where G is the shear modulus, $\boldsymbol{\ell}$ is the strain rate, and $\boldsymbol{\Omega}$ is the rotation tensor:

$$\ell^{\alpha\beta} = \frac{1}{2}\left(\frac{\partial v^{\alpha}}{\partial x^{\beta}} + \frac{\partial v^{\beta}}{\partial x^{\alpha}}\right), \quad \Omega^{\alpha\beta} = \frac{1}{2}\left(\frac{\partial v^{\alpha}}{\partial x^{\beta}} - \frac{\partial v^{\beta}}{\partial x^{\alpha}}\right). \tag{5}$$

The damaged stress tensor. We adopt a modified form of Grady-Kipp model [16] to predict rock damage based on the local stress history and flaw distribution. This model is based on the Weibull distribution of flaws. As many other models, the modified Grady-Kipp damage model defines a scalar parameter D such that $0 \leq D \leq 1$ to characterize the volume-averaged micro-fracture of the volume of material based on the strain history. Material with $D = 0$ is undamaged and is able to transmit the full tensile load, whereas material with $D = 1$ is fully damaged and cannot transmit any tensile load, thus creating a partial macro-crack [10].

Specifically, the damaged stress $\boldsymbol{\sigma}_d$ and the undamaged stress $\boldsymbol{\sigma}$ are related as follows. Let the principal components of $\boldsymbol{\sigma}$ be σ^1 and σ^2 and the corresponding principal directions be $\mathbf{n}^1$ and $\mathbf{n}^2$. Then $\boldsymbol{\sigma}$ can be written as

$$\boldsymbol{\sigma} = \sum_{a=1}^{2} \sigma^a \mathbf{n}^a \otimes \mathbf{n}^a.$$

The principal components of $\boldsymbol{\sigma}_d$ are then obtained from

$$\sigma_d^a = \begin{cases} (1-D)\sigma^a, & \text{if } \sigma^a \geq 0, \\ \sigma^a, & \text{otherwise,} \end{cases}$$

for $a = 1, 2$. In other words, tensile stresses are only partially transmitted through damaged materials while compressive stresses are totally transmitted.

As a result,

$$\boldsymbol{\sigma}_d = \sum_{a=1}^{2} \sigma_d^a \mathbf{n}^a \otimes \mathbf{n}^a.$$

At each point, the damage $D(t)$ evolution is given by

$$\frac{dD^{1/3}}{dt} = \begin{cases} C\varepsilon_{\text{eff}}^{m/3}, & \text{if } t > t_{\text{onset}}, \\ 0, & \text{otherwise,} \end{cases} \tag{6}$$

where we have absorbed the material parameters in [16, 10] into a single one, C. The effective tensile strain ε_{eff} is given by Melosh et al. [18]:

$$\varepsilon_{\text{eff}} = \sigma_{\max} \Big/ \left(K + \frac{4}{3} G \right), \tag{7}$$

where $\sigma_{\max} = \max\{0, \sigma^1, \sigma^2\}$ is the maximum positive principal stress, and K is the bulk modulus of the material.

In the subsequent calculations, the onset time t_{onset} is defined as the first instant when $\varepsilon_{\text{eff}} \geq \varepsilon_{\min}$, where

$$\varepsilon_{\min} := \left(\frac{m_j}{\rho_j} k \right)^{-1/m},$$

where m_j and ρ_j are the particle mass and density to be introduced later, and k and m are parameters of the Grady-Kipp model.

2.2.2 The explosive gas

For the explosive gas, as the isotropic pressure is much larger than components of viscous shear stress, the viscous shear stress can be neglected, hence

$$\sigma^{\alpha\beta} = -p\delta^{\alpha\beta},$$

where the hydrodynamic pressure p is related to the internal energy e according to the standard Jones-Wilkins-Lee (JWL) equation of state [19]:

$$p = A \left(1 - \frac{\omega\eta}{R_1} \right) e^{\frac{R_1}{\eta}} + B \left(1 - \frac{\omega\eta}{R_2} \right) e^{\frac{R_2}{\eta}} + \omega\eta\rho_0 E, \tag{8}$$

where $\eta = \rho/\rho_0$ is the ratio of the density of the explosive gas to the initial density of the original explosive. Parameters A, B, R_1, R_2 and ω are coefficients obtained by fitting experimental data, and E is the initial internal energy of the high explosive per unit mass. Values of the corresponding coefficients are listed in Table 1.

Table 1: Parameters used in the JWL equation for TNT.

Parameter	ρ_0	A	B	R_1	R_2	ω	E
Quantity	1630	317.2	3.21	4.15	0.95	0.30	4290
Unit	$\text{kg} \cdot \text{m}^{-3}$	GPa	GPa				$\text{kJ} \cdot \text{kg}^{-1}$

2.3 Coupling conditions

At the interface, the velocity and pressure of the two phases are continuous, i.e.,

$$v^{\alpha}_{\text{gas}} = v^{\alpha}_{\text{rock}}, \quad p_{\text{gas}} = p_{\text{rock}}.$$

3 SMOOTHED PARTICLE HYDRODYNAMICS METHOD

3.1 Basic concept

We start by representing an arbitrary function $f(\mathbf{x})$ with discrete values at particles located at $\mathbf{x}_1, \ldots, \mathbf{x}_N$, denoted $f_1, \ldots, f_N$:

$$f(\mathbf{x}) = \sum_{j=1}^{N} \frac{m_j}{\rho_j} f_j W(\mathbf{x} - \mathbf{x}_j, h), \tag{9}$$

where m_j and ρ_j denote the mass and density of particle j, respectively, h is the smooth length, and W, usually called a *kernel* or *kernel function*, is a smoothing function representing a weighted contribution of the particles. This smoothing function should satisfy some basic requirements. Detailed discussions on the smoothing function, its basic requirements and constructing conditions can found in [15]. In this work, we choose the Gaussian kernel

$$W(\mathbf{r}, h) = W(r, h) = \alpha_d \exp\left[-(r/h)^2\right],$$

where $r := |\mathbf{r}|$ and α_d is a dimension-dependent constant related to the smoothing length. In 2D, $\alpha_d = (\pi h^2)^{-1}$.

Any partial derivative of $f(\mathbf{x})$ can then be represented as:

$$\frac{\partial f(\mathbf{x})}{\partial x^{\beta}} \doteq \sum_{j=1}^{N} \frac{m_j}{\rho_j} f_j \frac{\partial^{\text{c}} W(\mathbf{x} - \mathbf{x}_j, h)}{\partial x^{\beta}}, \tag{10}$$

where $\partial^{\text{c}}/\partial x^{\beta}$ is an approximation to $\partial/\partial x^{\beta}$. This approximation involves a kernel correction, which we will elaborate in Section 3.2.

Specializing (9) and (10) to $\mathbf{x} = \mathbf{x}_i$ and using $f_i \doteq f(\mathbf{x}_i)$, we have, for $i = 1, \ldots, N$,

$$f_i \doteq \sum_{j=1}^{N} \frac{m_j}{\rho_j} f_j W_{ij}, \quad \left(\frac{\partial f}{\partial x^{\beta}}\right)_i \doteq \sum_{j=1}^{N} \frac{m_j}{\rho_j} f_j \frac{\partial^{\text{c}} W_{ij}}{\partial x_i^{\beta}}, \tag{11}$$

where

$$W_{ij} := W(\mathbf{x}_i - \mathbf{x}_j, h) = W(|x_i - x_j|, h).$$

Ideally, by applying (11) to $f(\mathbf{x}) = 1$, we have the approximate consistency equations,

$$\sum_{j=1}^{N} \frac{m_j}{\rho_j} W_{ij} \doteq 1, \quad \sum_{j=1}^{N} \frac{m_j}{\rho_j} \frac{\partial^{\text{c}} W_{ij}}{\partial x_i^{\beta}} \doteq 0. \tag{12}$$

where $i = 1, \ldots, N$ and $\beta = 1, 2$.

3.2 Kernel gradient correction

In this paper, we improve the kernel gradient in SPH approximations with a kernel gradient correction (KGC) technique [20]. In the KGC technique, a modified or corrected kernel gradient is obtained by multiplying the original kernel gradient with a local reversible matrix $\boldsymbol{L}_i$, which is obtained from Taylor series expansion method. In 2D, the new kernel gradient of the smoothing function $\nabla_i^{\mathrm{c}} W_{ij}$ can be obtained as follows

$$\nabla_i^{\mathrm{c}} W_{ij} := \boldsymbol{L}_i \nabla_i W_{ij}, \quad \boldsymbol{L}_i := \left(\sum_j \frac{m_j}{\rho_j} \begin{bmatrix} x_{ji}^1 \dfrac{\partial W_{ij}}{\partial x_i^1} & x_{ji}^2 \dfrac{\partial W_{ij}}{\partial x_i^1} \\ x_{ji}^1 \dfrac{\partial W_{ij}}{\partial x_i^2} & x_{ji}^2 \dfrac{\partial W_{ij}}{\partial x_i^2} \end{bmatrix} \right)^{-1}, \tag{13}$$

where

$$\nabla_i^{\mathrm{c}} W_{ij} := \begin{Bmatrix} \partial^{\mathrm{c}} W_{ij}/\partial x_i^1 \\ \partial^{\mathrm{c}} W_{ij}/\partial x_i^2 \end{Bmatrix}, \quad \nabla_i W_{ij} := \begin{Bmatrix} \partial W_{ij}/\partial x_i^1 \\ \partial W_{ij}/\partial x_i^2 \end{Bmatrix}.$$

3.3 SPH discretization of motion equations

We will obtain SPH discretization equations by applying SPH approximations (11) along with the approximate consistency equations (12) to (1). For stability concerns, we introduce artificial viscosity Π_{ij} and artificial heat H_i [15]. With these, the SPH discretization equations become

$$\begin{cases} \dfrac{Dx_i^\alpha}{Dt} = v_i^\alpha, \\ \dfrac{Dv_i^\alpha}{Dt} = -\displaystyle\sum_{j=1}^N m_j \left(\frac{\left(\sigma_d^{\alpha\beta}\right)_i}{\rho_i^2} + \frac{\left(\sigma_d^{\alpha\beta}\right)_j}{\rho_j^2} + \Pi_{ij} \right) \frac{\partial^{\mathrm{c}} W_{ij}}{\partial x_i^\beta}, \\ \dfrac{D\rho_i}{Dt} = \rho_i \displaystyle\sum_{j=1}^N \frac{m_j}{\rho_j} \left(v_i^\beta - v_j^\beta \right) \frac{\partial^{\mathrm{c}} W_{ij}}{\partial x_i^\beta}, \\ \dfrac{De_i}{Dt} = \dfrac{1}{2} \displaystyle\sum_{j=1}^N m_j \left(\frac{p_i}{\rho_i^2} + \frac{p_j}{\rho_j^2} + \Pi_{ij} \right) \left(v_i^\beta - v_j^\beta \right) \frac{\partial^{\mathrm{c}} W_{ij}}{\partial x_i^\beta} + \frac{1}{\rho_i} S_i^{\alpha\beta} \ell_i^{\alpha\beta} + H_i, \end{cases} \tag{14}$$

where subscripts i and j denote particle numbers, and all approximate equal signs "$\doteq$" are replaced with equal signs for brevity. The derivation of all equations of (14) is straightforward except for the last one, for which we refer the reader to [15, Chapter 4].

For particle i, the SPH equations for the strain rate $\boldsymbol{\ell}_i$ and the rotation tensor $\boldsymbol{\Omega}_i$

defined in (5) are:

$$\ell_i^{\alpha\beta} = \frac{1}{2}\sum_j \frac{m_j}{\rho_j}\left[\left(v_j^\alpha - v_i^\alpha\right)\frac{\partial^{\mathrm{c}} W_{ij}}{\partial x_i^\beta} + \left(v_j^\beta - v_i^\beta\right)\frac{\partial^{\mathrm{c}} W_{ij}}{\partial x_i^\alpha}\right], \tag{15}$$

$$\Omega_i^{\alpha\beta} = \frac{1}{2}\sum_j \frac{m_j}{\rho_j}\left[\left(v_j^\alpha - v_i^\alpha\right)\frac{\partial^{\mathrm{c}} W_{ij}}{\partial x_i^\beta} - \left(v_j^\beta - v_i^\beta\right)\frac{\partial^{\mathrm{c}} W_{ij}}{\partial x_i^\alpha}\right]. \tag{16}$$

3.4 Artificial viscosity and artificial heat

The artificial viscosity is used in SPH method to stabilize the numerical scheme, prevent particle penetration and capture shock waves. In this paper, we employ the standard artificial viscosity [15]:

$$\Pi_{ij} = \begin{cases} \dfrac{-\alpha_\Pi \overline{c}_{ij}\phi_{ij} + \beta_\Pi \phi_{ij}^2}{\overline{\rho}_{ij}}, & \mathbf{v}_{ij}\cdot\mathbf{x}_{ij} < 0, \\ 0, & \text{otherwise}, \end{cases} \tag{17}$$

where

$$\phi_{ij} := \frac{\overline{h}_{ij}\mathbf{v}_{ij}\cdot\mathbf{x}_{ij}}{|\mathbf{x}_{ij}|^2 + \left(0.1\overline{h}_{ij}\right)^2}, \quad \mathbf{v}_{ij} := \mathbf{v}_i - \mathbf{v}_j, \quad \mathbf{x}_{ij} := \mathbf{x}_i - \mathbf{x}_j,$$
$$\overline{c}_{ij} := \frac{1}{2}(c_i + c_j), \quad \overline{\rho}_{ij} := \frac{1}{2}(\rho_i + \rho_j), \quad \overline{h}_{ij} := \frac{1}{2}(h_i + h_j).$$

In the above equations, α_Π and β_Π are constants that are typically set around 1.0. Symbol c_i denotes the longitudinal wave speed of particle i. The viscosity term associated with α_Π produces a bulk viscosity, while the second term associated with β_Π, which is intended to suppress particle interpenetration at high velocity, is similar to the von Neumann-Richtmyer artificial viscosity.

To compensate the heat due to artificial viscosity, we put in the system the following artificial heat expression:

$$H_i = 2\sum_{j=1}^{N} \frac{\overline{q}_{ij}}{\overline{\rho}_{ij}} \frac{e_i - e_j}{|\mathbf{x}_{ij}|^2 + \left(0.1\overline{h}_{ij}\right)^2}\mathbf{x}_{ij}\cdot\nabla_i^{\mathrm{c}} W_{ij},$$

where

$$\overline{q}_{ij} := q_i + q_j, \quad q_i := \alpha_\Pi h_i \rho_i c_i |\nabla\cdot\mathbf{v}_i| + \beta_\Pi h_i^2 \rho_i |\nabla\cdot\mathbf{v}_i|^2.$$

3.5 Interaction between phases

The summation in (14) only takes into account particles of the same species. Between different particles, in this case between a solid particle and a gas particle, a force is

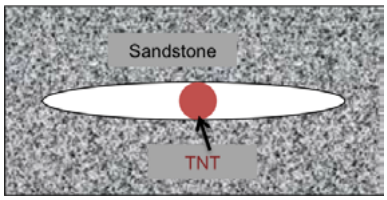

Figure 1: The initial configuration of the numerical example, which consists of a sandstone of a rectangular shape with an elliptical void.

applied to model their interaction. The force on particle i by particle j is expressed as a Lenard-Jones type interaction:

$$\mathbf{f}_{ij} = \begin{cases} D_{\text{int}} \left[(r_0/r_{ij})^4 - (r_0/r_{ij})^2 \right] (\mathbf{x}_{ij}/r_{ij}^2), & \text{if } r_{ij} < r_0, \\ 0, & \text{otherwise,} \end{cases}$$

where D_{int} is a parameter proportional to the square of the largest velocity, and r_0 is on the scale of the initial spacing of the particles.

3.6 Time integration

We use the leap-frog (LF) method to advance in time because it is efficient and needs to store only a small amount of memory [21]. As a typical explicit method, it is subject to the Courant-Friedrich-Levy (CFL) condition for stability, which typically results in a time step proportional to the smoothing lengths h. In this work, the time step is taken as,

$$\Delta t = \min_i \frac{\xi h_i}{\nabla \cdot \mathbf{v}_i + c_i + 1.2(\alpha_\Pi c_i + \beta_\Pi |\nabla \cdot \mathbf{v}_i|)},$$

where $\xi = 0.3$ is the Courant number.

4 NUMERICAL EXAMPLES

As a preliminary study, we model a typical sandstone of a rectangular shape with an elliptical void. The size of the rectangle is 2m×1m and the major and minor axes of the void are 1.6m and 0.2m, respectively. The sandstone has a bulk modulus of 12.2 GPa, a shear modulus of 2.67GPa, and a density of 2300kg/m^3. Here the Weibull damage parameters involved in the damage model are $k = 6.35 \times 10^{46}$ and $m = 12.8$, respectively. As a result, the parameter C in the Grady-Kipp model takes the value of 4.604×10^{18}. The geometry and material properties of the rock are from [22]. The boundaries of the rock are free, which will be changed to a fixed boundary in the near future. The specimen domain was discretized using particles in an initial rectangular grid pattern with a spacing of 0.02m.

Figure 1 illustrates the initial configuration, Figure 2 and Figure 3 show the snapshots of the damage parameter at different times with free boundary and fixed boundary respectively. We can see that damage originates from the part of the rock closest to the

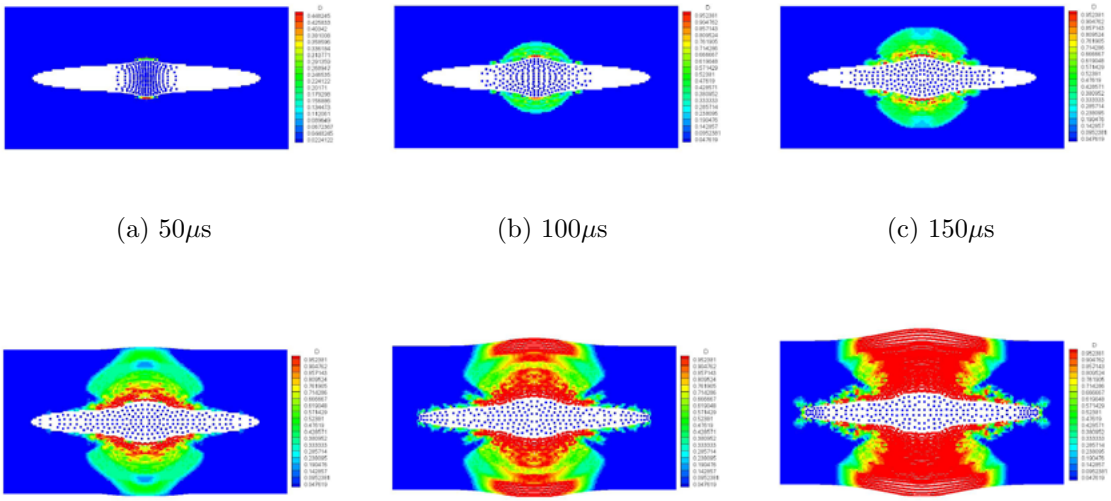

(a) 50μs (b) 100μs (c) 150μs

(d) 200μs (e) 250μs (f) 300μs

Figure 2: Snapshots of the damage parameter D at various times with free boundary. We can see that damage originates from the part of the rock closest to the explosive and then the tips of the void due to expansion of explosive gas. There is spalling at upper and down boundary.

explosive and then the tips of the void due to expansion of explosive gas. In the example with free boundary, the spalling is accompanied at top and bottom of rock mass.In the example with fixed boundary, obviously we can see spalling and collapse of inner domain of the rock mass and the artifact due to the fixed boundary, which we will change to a non-reflected boundary in the near future.

REFERENCES

[1] W. I. Duvall and D. E. Fogelson. *Review of Criteria for Estimating Damage to Residences from Blasting Vibrations*. U.S. Dept. of the Interior, Bureau of Mines, 1962.

[2] U. Langefors and B. Khilstrom. *The Modern Technique of Rock Blasting*. Wiley, New York, 2nd edition, 1973.

[3] J. Song and K. Kim. Micromechanical modeling of the dynamic fracture process during rock blasting. *Int. J. Rock Mech. Min. Sci. & Geomech. Abstr.*, 33:387–394, 1996.

[4] F. V. Donzé, J. Bouchez, and S. A. Magnier. Modeling fractures in rock blasting. *Int. J. Rock Mech. Min. Sci.*, 34:1153–1163, 1997.

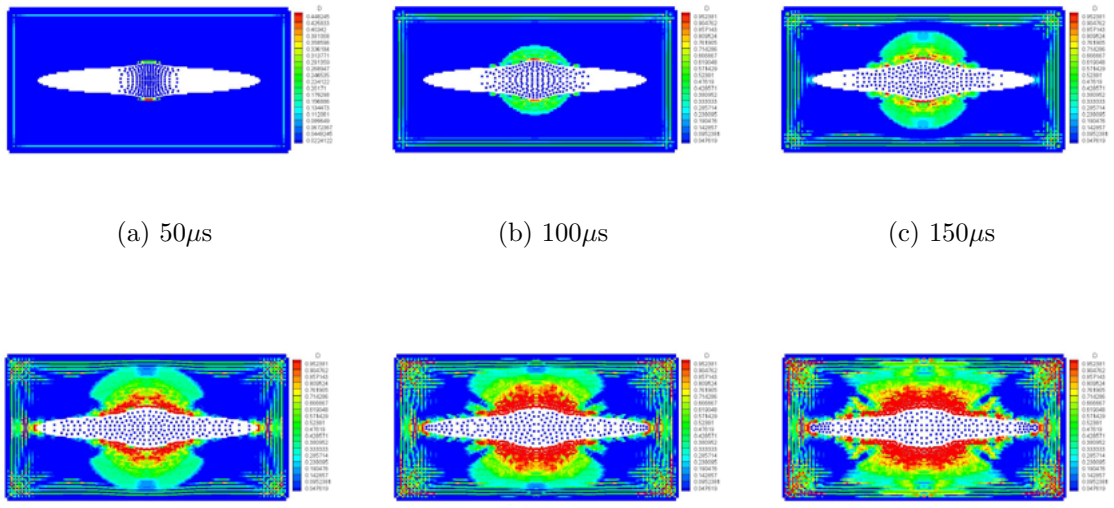

(a) 50μs (b) 100μs (c) 150μs

(d) 200μs (e) 250μs (f) 300μs

Figure 3: Snapshots of the damage parameter D at various times with fixed boundary. We can see that damage originates from the part of the rock closest to the explosive and then the tips of the void, as expected. Nevertheless, we also see the artifact due to the fixed boundary, which we will change to a non-reflected boundary in the near future.

[5] Y. Q. Zhang, H. Hao, and Y. Lu. Anisotropic dynamic damage and fragmentation of rock materials under explosive loading. *Int. J. Eng. Sci.*, 41:917–929, 2003.

[6] Z. L. Wang, Y. C. Li, and R. F. Shen. Numerical simulation of tensile damage and blast crater in brittle rock due to underground explosion. *Int. J. Rock Mech. Min. Sci.*, 44:730–738, 2007.

[7] G. W. Ma and X. M. An. Numerical simulation of blasting-induced rock fractures. *Int. J. Rock Mech. Min. Sci.*, 45:966–975, 2008.

[8] Q. Zhu, D. Kondo, J. Shao, and V. Pensee. Micromechanical modelling of anisotropic damage in brittle rocks and application. *Int. J. Rock Mech. Min. Sci.*, 45:467–477, 2008.

[9] S. W. Lee, K. H. Park, and J. G. Lee. Blast-induced damage identification of rock mass using wavelet transform analysis. *Procedia Engineering*, 14:3142–3146, 2011.

[10] D. E. Grady and M. E. Kipp. Continuum modelling of explosive fracture in oil shale. *Int. J. Rock Mech. Min. Sci. & Geomech. Abstr.*, 17:147–157, 1980.

[11] L. M. Taylor, E. P. Chen, and J. S. Kuszmaul. Micro-crack induced damage accumulation in brittle rock under dynamic loading. *Comp. Meth. Appl. Mech. Eng.*, 55:301–320, 1986.

[12] G. R. Johnson and T. J. Holmquist. An improved computational constitutive model for brittle materials. In S. C. Schmidt, J. W. Shaner, G. A. Samara, and M. Ross, editors, *High Pressure Science and Technology–1993*, pages 981—984. AIP Press, Woodbury, NY, 1994.

[13] I. A. Onederra, J. K. Furtney, E. Sellers, and S. Iverson. Modelling blast induced damage from a fully coupled explosive charge. *Int. J. Rock Mech. Min. Sci.*, 58:73–84, 2013.

[14] L. B. Lucy. A numerical approach to the testing of the fission hypothesis. *The Astronomical Journal*, 82:1013–1024, 1977.

[15] G. R. Liu and M. B. Liu. *Smoothed Particle Hydrodynamics: A Meshfree Particle Method*. World Scientific, Singapore, 2003.

[16] R. Das and P. W. Cleary. Effect of rock shapes on brittle fracture using smoothed particle hydrodynamics. *Theo. Appl. Frac. Mech.*, 53:47–60, 2010.

[17] G. Yang, X. Han, and D. A. Hu. Computer simulation of two-dimensional linear-shaped charge jet using smoothed particle hydrodynamics. *Eng. Computation*, 28:58–75, 2011.

[18] H. J. Melosh, E. V. Ryan, and E. Asphaug. Dynamic fragmentation in impacts: Hydrocode simulation of laboratory impacts. *J. Geophys. Res.*, 97:14735–14759, 1992.

[19] E. L. Lee, H. C. Hornig, and J. W. Kury. Adiabatic expansion of high explosive detonation products. Technical report, Lawrence Radiation Lab, Univ. California, Livermore, 1968.

[20] J. R. Shao, H. Q. Li, G. R. Liu, and M. B. Liu. An improved SPH method for modeling liquid sloshing dynamics. *Comput. Struct.*, 100–101:18–26, 2012.

[21] M. B. Liu, G. R. Liu, Z. Zong, and K. Y. Lam. Computer simulation of high explosive explosion using smoothed particle hydrodynamics methodology. *Comput. Fluids*, 32:305–322, 2003.

[22] S. Karekal, R. Das, L. Mosse, and P. W. Cleary. Application of a mesh-free continuum method for simulation of rock caving processes. *Int. J. Rock Mech. Min. Sci.*, 48:703–711, 2011.